Case Studies in Construction Materials 15 (2021) e00695

Contents lists available at ScienceDirect

Case Studies in Construction Materials

journal homepage: www.elsevier.com/locate/cscm

Case study

Relationship between damage and structural vulnerability in historical heritage: Case study of San Fernando de Bocachica Fort, Cartagena de Indias

Arnoldo Berrocal-Olave [a], Manuel Saba [a,*], Juan C. Olmo-Garcia [b]

[a] Research Group Structures, Constructions and Heritage (ESCONPAT), Universidad de Cartagena, Av. del Consulado Calle 30 # 48-152, Cartagena de Indias, Colombia

[b] Department of Architectural Graphic Expression and Engineering PAIDI Group HUM-222 (Andalusian Architectural and Urban Heritage) Universidad de Granada, Plaza Campo del Principe S/N CP, 18071 Granada, Spain

ARTICLE INFO

Keywords:
Preservation of monuments
Historical heritage
Structural vulnerability
Graphic representation of historical monuments

ABSTRACT

The restoration process for historical heritage is complex and consists of several steps. In the professional field, the evaluation of the structural vulnerability of a historical monument often does not include an evaluation of its previous damage. It is important to understand the degradation phenomena to properly interpret the results of structural analysis and make better decisions for the maintenance and structural reinforcement.

In the present study, a seismic vulnerability assessment with a linear dynamic analysis was carried out at San Fernando de Bocachica Fort. In addition, structural damage and deterioration types were categorized and mapped. Finally, a comparison between structure stress distribution and damage analysis is proposed. A marked relationship between structural overstress and structural decay is noted, which makes this methodology a valuable tool that could be implemented for the more effective maintenance of historical heritage around the world. The fort presents severe deterioration, highlighting the need for immediate intervention to preserve its aesthetic and structural stability.

1. Introduction

Historical monuments are invaluable and represent a relevant part of the history and culture of a country and of humanity as a whole [12,29,33]. Each historical structure requires a specific approach and a deep knowledge of its history, materials, construction phases, and restoration processes over time [36]. They are extremely vulnerable to seismic actions because, generally, the original construction techniques were mostly dedicated to preserving the balance against vertical gravitational loads. Additionally, these structures are constantly exposed to deterioration by weathering. For this reason, many interventions to preserve their integrity are often needed, which are not often off record [25].

Baraccani et al. [2] present a preliminary assessment of the structural "health" of the Cathedral of Modena (Italy) making use of a multi-disciplinary multi-analysis approach, capable of providing an *integrated knowledge* of the monument. Different analyses have

* Corresponding author.
E-mail addresses: aberrocalo@unicartagena.edu.co (A. Berrocal-Olave), msaba@unicartagena.edu.co (M. Saba), jolmog@ugr.es (J.C. Olmo-Garcia).

https://doi.org/10.1016/j.cscm.2021.e00695
Received 23 April 2021; Received in revised form 27 August 2021; Accepted 8 September 2021
Available online 20 September 2021
2214-5095/© 2021 The Authors. Published by Elsevier Ltd. This is an open access article under the CC BY-NC-ND license (http://creativecommons.org/licenses/by-nc-nd/4.0/).

Fig. 1. View of the San Fernando de Bocachica Fort.
Source: http://www.dronestagr.am/san-fernando-de-bocachica-2/.

been conducted on the global structure of the masonry fabric as well as on the local response of the single masonry walls and other significant structural elements, in order to identify the main static vulnerabilities. Construction phases, differential settlements and interaction with close structures are the key factors to be considered for the structural assessment, supported by the structural monitoring, as an essential component of the integrated studies when exploring the long-term performances.

As discussed by several authors, [23,25,4], the systematic process of observation, monitoring, and data recording over a period of time to characterize the health status of structures and detect any possible changes due to the occurrence of damage is known as structural health monitoring (SHM).

SHM represents a diagnostic and control tool and plays a fundamental role in the entire conservation process ([8,21]; M. G. [24,35,34]). Decay process studies on historical monuments in this direction are often found in the literature [13,30]. In the recent research on the two Towers of Bologna (Italy), Baraccani et al. [1] introduce an innovative time-domain approach for the analysis and interpretation of large amount of data from long-term static monitoring of historical masonry structures to analyze data from the SHM system. On the other hand, Makoond et al. [22] propose a static structural health monitoring and automated data analysis procedures applied to the diagnosis of a complex medieval masonry monastery. In both cases the usefulness of those approaches in a broader decision-making framework is highlighted.

However, most studies are limited to damage analysis or structural analysis, with different levels of complexity [31,37,7]. The study and monitoring of structural decay processes should be conducted in parallel with a structural analysis. The structural vulnerability of a structure can be observed to be reflected in the type of damage and distribution. Therefore, an accurate diagnosis of structure damage is crucial to the implementation of appropriate measures in their intervention in order to improve the efficiency of the restoration and conservation process [23].

Furthermore, in developing countries SHM often it is not possible due to lack of funds and logistic problems related to the safety of installed devices. Therefore, it is necessary to resort to alternative techniques.

This study focuses on Cartagena de Indias, Colombia. The city is characterized by a set of fortresses, bastions, monuments, and defensive walls, being part of the world heritage list according to the United Nations Educational, Scientific and Cultural Organization (UNESCO) since 1984 [40]. This due to the important historical, cultural, architectural, and military engineering value that it represents. In particular, San Fernando de Bocachica Fort is an important piece of that legacy, and it is located on the island of Tierrabomba in front of the San José Battery (Fig. 1).

This fort is an 18th century Hispanic construction, with a purely defensive character, essential for the survival of the city in the period of the Spanish Crown in Colombia, [39]. Three centuries after its construction, it continues to be of great importance for the city of Cartagena de Indias from a historical–architectural point of view and as a tourist attraction, with tourism being the second source of income for the city after industry [28].

This structure over the years has shown some deterioration due to the tropical environment, high temperatures, humidity, salinity, the continuous effect of waves, and the lack of conservation and maintenance, among other factors. For this reason, the objective of this work was to identify the relationship among the decay process, damage, and structural behavior. This work aims to serve as a reference for the protection of Cartagena's heritage and similar cultural heritage.

2. Methodology

To facilitate the analysis, the fort was divided into 6 sectors whose names correspond to the letters from A to F. Furthermore, Sector

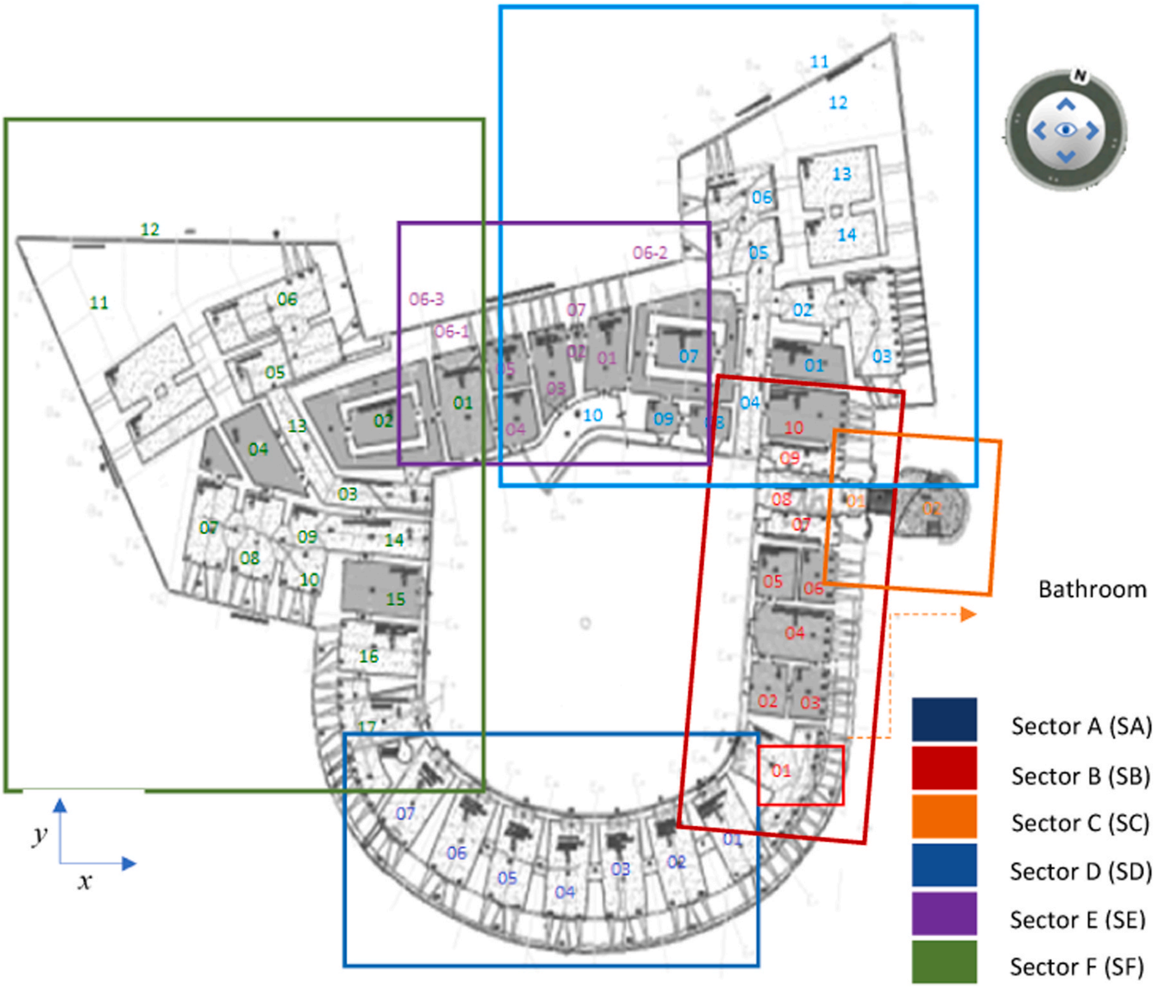

Fig. 2. Plan of San Fernando Fort divided by sectors.

A was divided into 5 parts, Sector B into 10 parts, Sector C into 2 parts, Sector D into 12 parts, Sector E into 7 parts, and, finally, Sector F into 12 parts (Fig. 2).

The decay phenomena and processes are described using the glossary proposed by the International Scientific Committee for Stone (ISCS) and the International Council on Monuments and Sites (ICOMOS) [17]. The ICOMOS-ISCS glossary was created in order to unify the terminology in studies on the alteration and conservation of stone, which is a crucial issue in the conservation of monuments. The glossary highlights 5 main groups: cracks and deformations, detachments, features induced by material loss, discoloration and deposit, and biological colonization, which are divided into sub-categories. Moisture content represents neither a decay phenomenon nor a process itself. However, as it triggers several deterioration processes, it was considered in the present study.

The list of the decay phenomena and processes found in the in-situ inspection was reported with 48 records, including the name of the fortification, divisions made, a plan view of the structure, and graphic–photographic evidence. After this, the decay condition of each evaluated part was qualitatively categorized as good, fair, poor, or bad, according to the in-situ visit, corresponding to the colors green, yellow, orange, and red, respectively.

The risk condition was evaluated according to the localization of considered area and the importance of its functionality to the local and overall structural stability. It was categorized as low, moderate, serious, or very serious, following the same chromatography as that described above.

Furthermore, each record reports on whether the decay identified affects the structure's stability or its aesthetic. Fig. 3 shows a completed record of an inspection of San Fernando as an example.

2.1. Materials

The materials found in San Fernando Fort were limestone, military brick, lime-based mortar, and what is locally called colonial concrete (mixed concrete). This is made up of fragments of limestone, coral, and pumice and fragments of tiles or bricks, bonded with

SAN FERNANDO DE BOCACHICA FORT		Date:	23/08/2020
Tipology:	Vault		
Location		Code:	Record N°
		SC-01	0-14

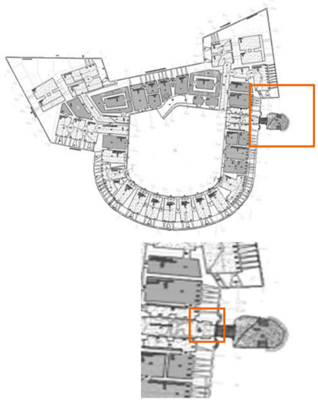

Damages:

Damage group	Type of Damage	Damage Subtype
Features induced by Material loss	Features induced by Material loss	Loss of Mortar

Condition:

Condition	Clasification	Color condition
Fair	1	

Risk:

Grade	Clasification	Sorting by color
Moderate	1	

Affectation:

Safety Aesthetics

OBSERVATIONS:
Loss of mortar in the joints (Top photo).

Alveolization with cavities greater than 2 cm, disjunction of films, disintegration of the stone structure (Central photo).

Fracturing and detachment of stone material from the structure is observed (Bottom photo).

POSSIBLE CAUSES:
Runoff water and chemical factors that have disintegrated the mortar.

Limestone corrosion, mechanical aggression, wind erosion and rainwater.

Impact aggression and weathering.

Fig. 3. Example of the San Fernando inspection record [3].

Fig. 4. Materials of San Fernando de Bocachica Fort. a) Limestone; b) brick; c) plastered limestone; d) mixed concrete.b).

Table 1
Material mechanical properties.

Material	Location in the structure	E (MPa)	Bulk density (kg/m$^{3)}$	Strength (MPa)		
				Rc	Rt	S
Limestone	Scarp	1956.0	2280.0	2.55	0.12–0.25	0.31
Mixed concrete	Internal, external walls and ramp	618.0	1535.0	0.82	0.04–0.08	0.17
Plastered limestone	Base vaults and low battery	10,981.9	2730.0	5.61	0.28–0.56	1.55
Military brick	Key to the vaults and ramp	2780.9	1685.14	3.70	0.18–0.37	1.27

E = elastic modulus; Rc = uniaxial compressive strength; Rc = uniaxial tensile strength; S = shear strength.

mortar (Fig. 4a–d).

For limestone, elastic modulus was obtained from cylinders extracted in situ, while the Poisson's ratio was obtained theoretically, according to title D 5.2 of the Colombian construction standard (NSR-10, for its initials in Spanish).

The military brick in San Fernando Fort is found in various proportions; the most common is the so-called Tolete brick measuring 0.30 × 0.15 × 0.05 m, and it is of excellent quality in terms of clay and firing. This material was tested in non-destructive tests carried out by means of a smith's hammer following the NTC 4205 Colombian standard. The brick works were immersed within a matrix of mortar. Therefore, 23 brick walls were tested for compression and axial deformation to determine the elastic modulus, according to ASTM E111 standards. Poisson's ratio was obtained as mentioned above for limestone (Table 1).

Regarding the mixed concrete, five walls of 0.3 × 0.20 × 0.3 m were extracted in buildings with similar construction techniques

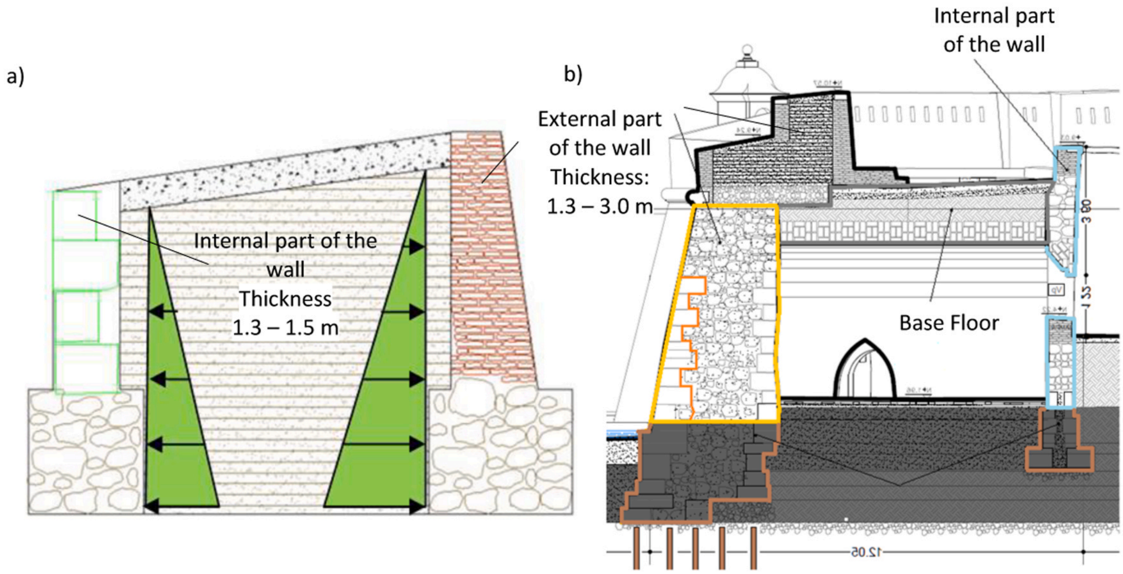

Fig. 5. a) Generic section of the Fort; b) Curtain and bastion construction system near to water bodies.

Table 2
Summary of load combination considered.

Foundation condition	Cases	Loads considered
1) Embedded structure	Case 1	Filling Thrust; Live Load, Dead Load, Sea Waves
	Case 2	Filling Thrust, Live Load, Dead Load, Sea Waves, Earthquake with Limited Security (Existing Structure)
	Case 3	Filling Thrust, Live Load, Dead Load, Sea Wave, Earthquake with Design Spectrum Equivalent to a New Structure
2) Soil-structure interaction	Case 4	Filling Thrust, Live Load, Dead Load, Sea Waves
	Case 5	Filling Thrust, Live Load, Dead Load, Sea Waves, Earthquake with Limited Security (Existing Structure)
	Case 6	Filling Thrust, Live Load, Dead Load, Sea Wave, Earthquake with Design Spectrum Equivalent to a New Structure

Case 1 loads are equivalent to Case 4 loads, similarly for Case 2 to case 5 and Case 3 to Case 6. The only difference is the Foundation Condition. "Earthquake with Limited Security (Existing Structure)" refers to Colombian construction standard earthquake for existing structures with a reduced acceleration peak. "Design Spectrum" refers to Colombian construction standard earthquake for new structures (Fig. 5).

and quality of materials to those of San Fernando Fort [6]. The average value of compressive strength was obtained according to title D of NSR-10. Indirect tests, such as measurements through a sclerometer and ultrasound, were also carried out; however, they were not considered in the analysis since the tendency is to overestimate the strength of the materials.

The bulk density value was obtained by means of the weight and volume relationship for walls extracted in the old building of the Government of Bolívar (Claustro de Francisco), while the elastic modulus and Poisson's ratio were theoretically obtained in accordance with NSR-10 section D.5.2 (Table 1).

The decay conditions were considered for each section applying two reduction coefficients, to the values in Table 1, to obtain the design mechanical properties. Design quality (Φ_{dc}) and material decay (Φ_{md}) reduction coefficients were evaluated during the in-situ inspection of the structure.

2.2. FEM analysis

Additionally, a dynamic linear analysis of the structural behavior was undertaken using the finite element method (FEM) through the SAP2000® software. For the modeling of the external wall of the structure, solid elements were used, which are eight-node objects that are used to model structural systems in 3D. Each solid has six quadrilateral faces with a hinge at each corner. The nodes can be chosen to form wedges, tetrahedra, and other irregular volumes. This element is capable of resisting plane deformation, bending, and handling shear loads. On the other hand, the internal wall was modeled using a shell-thick element, applying Mindlin–Reissner's thick plate theory, [14,18] and using a node isoperimetric planar quadrilateral element capable of supporting planar deformation, bending, and handling shear loads.

The structure was modeled as a whole, nevertheless, due to the computational load, stress and strain results were extracted by section. In Fig. 5a schematic representation of the fortification is reported.

The load combination was applied in accordance with section B.2.3 of NSR-10 (Table 2.). Foundation conditions in this specific structure are unknown. Therefore, two different scenarios were considered, 1) embedded structure with an infinitely rigid floor and 2) with a soil–structure interaction. The reproduction of the soil-structure interaction is given by the allocation of springs in the supports

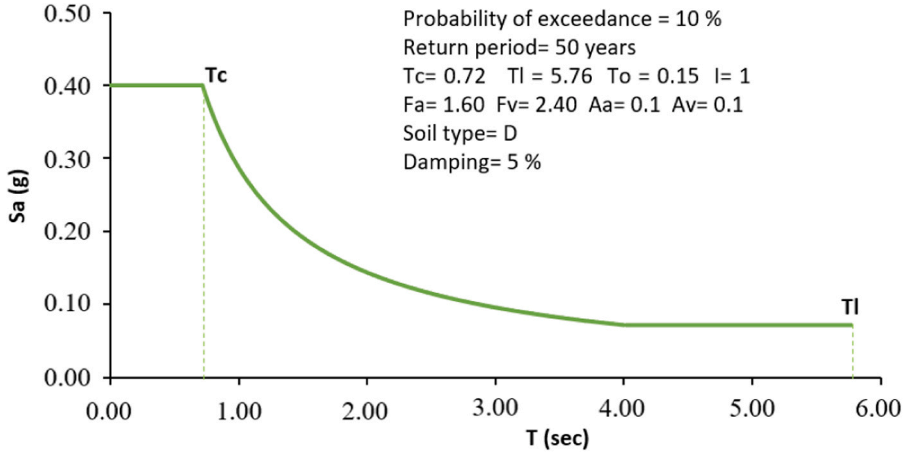

Fig. 6. Design spectrum for the NS according to NSR-10. I: coefficient of importance; Fa: amplification coefficient that affects the acceleration in the area of short periods; Fv: amplification coefficient that affects the acceleration in the area of intermediate periods.

Table 3
Applied Loads.

Applied Loads	Magnitude	Unit	Comments
Filling Thrust	7.42	t/m^2	Triangular load, with zero at the top h = 5.15
LL (Carga viva)	0.20	t/m^2	Due to Uniformly distributed load
Sea Waves (carga por oleaje)	0.61	t/m^2	Calculated pressures on the scarp
Earthquake with Limited Security (x and y Direction)	1567	t	
Earthquake Design Spectrum (x and y Direction)	3134	t	

All loads have to be considered horizontally applied to the wall façade; t = tons.

of the structure, whose stiffness characteristics are defined by the properties of the soil. Therefore, the theoretical determination of the stiffness of the soil becomes a fundamental part, since the reproduction of the real conditions to which the structures are subjected depends on it. For the purposes of this research, the stiffness values were established for the soil in the three directions. Stiffness constant in the z direction was assumed as 800 t/m^3, while for y and x directions as one third (267 t/m^3), according to previous research in the interested area, [11]. The foundations of the structures were modeled using a Shell element of SAP 2000 software V.16.1.1, this type of elements can only be added to the stiffness of the soil in terms of area - Surface spring [15,43].

Filling thrust, the thrust due the filling material behind the wall, was calculated applying the Rankine lateral thrust theory, (Fig. 5), [32,42]. For this, it was considered a specific weight value of 2.0 ton/m^3, a coefficient of internal friction of $\phi = 30^\circ$, active thrust constant K_a= 0.28 and cohesion coefficient of 1 t/m^2, taken from previous research, [11]. *Live load* is the active thrust in the wall as a result of the occupancy loads according to the NSR-10. *Dead load* is the structure's own weight (see Bulk density in Table 1). *Sea waves* represent the wave effect calculated according to George Sainflou's theory [10,20,38]. The pressure of the waves on vertical walls is composed of the hydrostatic pressure, which varies as the wave rises and falls along the wall; and by the dynamic pressure generated by the movement of the water particles. Height, length and depth of the wave were respectively 0.5 m, 25.5 m and 0.5 m.

Therefore, the three equilibrium conditions, the horizontal component of the earth thrust, overturning and bearing capacity, for the retaining wall were verified [27].

The seismic load in the x and y direction was calculated according to the response spectra (NSR-10). The design spectra were first determined under the consideration of earthquakes for new structures (NS) and then for limited safety structures (LSS) or existing structures. The difference between both design considerations lies in the values of the effective peak acceleration and effective peak velocity (Fig. 6). Both cases have a fundamental period (T) lower than the short period Tc of the spectrum (T = 0.24 in x and T = 0.24 in y). Therefore, the design acceleration Sa (g) was calculated with Eq. (1) (NSR-10), and the values adopted in the analysis were 0.40 g for NS and 0.20 for LSS (Fig. 6).

$$S_a = 2.5 A_a F_a I \quad (1)$$

The fundamental period of the structure is output data from the SAP2000 program after performing the modal analysis. It is necessary to consider that, according to NSR-10, all vibration modes that contribute in a significant way to the dynamic response of the structure must be included in the dynamic analysis, including at least 90% of the participating mass for x and y.

Applied loads are reported in Table 3.

Table 4
Decay evaluation in San Fernando Fort.

Sector		A					B								C	
Section		1	2	3	4	5	1	2-3	4	5-6	7	8	9	10	1	2
Causes	Cracks			X			X	X								
	Hair crack											X				
	Microkarst	X	X	X		X	X		X					X	X	X
	Alveolarization	X					X				X			X	X	X
	Missing part		X		X	X		X	X		X	X	X			
	Peeling	X	X	X	X	X	X	X	X	X	X	X	X	X	X	X
	Roughening	X	X	X	X	X							X	X		X
	Loss of matrix											X	X		X	
	Moist area	X	X	X	X	X	X	X	X	X	X	X	X	X	X	X
	Efflorescence	X					X									
Type of damage	Physical	X	X	X	X	X	X	X	X	X	X	X	X	X	X	X
	Mechanical			X			X	X								
	Chemical	X	X	X	X	X	X	X	X	X	X	X	X	X	X	X
	Biological	X		X	X	X	X	X						X		
Damage Condition		green	yellow	orange	yellow	yellow	red	orange	yellow	yellow	yellow	yellow	yellow	yellow	yellow	orange
Estimated risk		green	green	green	green	green	orange	yellow	green	green	green	green	green	green	yellow	yellow
Affect	Safety			X			X	X								X
	Aesthetic	X	X	X	X	X	X	X	X	X	X	X	X	X	X	X

Sector		D											
Section		1	2	3	4	5	6	7	8	9	10	11	12
Causes	Cracks											X	X
	Hair crack										X	X	X
	Microkarst				X		X		X		X	X	X
	Alveolarization				X				X			X	X
	Missing part	X										X	
	Peeling	X	X	X	X	X	X	X	X	X	X	X	X
	Roughening		X	X	X		X	X	X	X	X	X	X
	Loss of matrix							X				X	X
	Moist area	X	X	X	X	X	X			X			
	Efflorescence			X	X		X						
Type of damage	Physical	X	X	X	X	X	X	X	X	X	X	X	X
	Mechanical											X	
	Chemical	X	X	X	X	X	X	X		X			
	Biological	X		X		X	X			X			X
Damage Condition		yellow	green	yellow	yellow	yellow	yellow	yellow	yellow	yellow	yellow	orange	orange
Estimated risk		green	green	green	green	green	green	green	green	green	green	yellow	green
Affect	Safety											X	
	Aesthetic	X	X	X	X	X	X	X	X	X	X	X	X

Sector		E									F											
Section		1	2	3	4	5	6-1	6-2	6-3	7	1	2	3	4	5	6	7	8	9	10	11	12
Causes	Cracks						X		X	X											X	X
	Hair crack								X	X											X	X
	Microkarst	X	X	X	X	X	X	X		X	X	X			X	X					X	X
	Alveolarization	X			X		X	X		X	X	X				X						X
	Missing part	X	X	X	X	X			X	X												
	Peeling	X	X	X	X	X			X	X	X	X	X	X	X	X	X	X	X	X	X	X
	Roughening	X	X	X	X	X	X	X	X	X	X	X	X	X	X	X	X	X	X	X	X	X
	Loss of matrix				X		X	X	X	X		X		X							X	X
	Moist area	X	X	X	X	X	X	X			X		X	X	X	X	X	X	X	X		
	Efflorescence					X							X					X		X		
Type of damage	Physical	X	X	X	X	X		X	X	X	X	X	X	X	X	X	X	X	X		X	X
	Mechanical						X		X	X											X	X
	Chemical	X	X	X	X	X		X			X	X	X	X	X	X		X		X		
	Biological	X	X														X	X	X	X	X	X
Damage Condition		yellow	yellow	yellow	yellow	yellow	orange	orange	orange	orange	yellow	green	yellow	yellow	yellow	yellow	yellow	yellow	yellow	yellow	orange	orange
Estimated risk		green	green	green	green	green	yellow	yellow	yellow	yellow	green	green	green	green	green	green	green	green	green	green	yellow	yellow
Affect	Safety						X	X	X												X	X
	Aesthetic	X	X	X	X	X		X	X	X	X	X	X	X	X	X	X	X	X	X	X	X

Fig. 7. Deterioration of the plaster, green spots on the wall of the vault, and rising damp on the floor.

3. Results and discussion

The fort has been restored many times over the centuries, but no record of the specific interventions has been found. There are no flooded areas, and the overall structural behavior of the Fort is acceptable, despite some local criticalities to be considered.

The action of the waves on San Fernando de Bocachica Fort has generated the loss of a large part of the sandy material at the base of the structure, which probably caused differential settlements. Hidroconsultores [16] states that the loss of material in the San Fernando de Bocachica Fort occurs when the water tries to get out of the bay, producing water currents at the foot of the fort dragging the support material beneath the edge of the foundation.

The overall is-situ visit highlighted general widespread moisture content presence through walls and roofs, and inadequate drainage systems.

It is unknown the level of consolidation of the ground foundations and structure monitoring was not the objective of this study, although further studies are planned in this matter.

A summary of the parameters recorded in the decay evaluation sheets of San Fernando Fort is shown in Table 4. All sections of the fort and the types of damage (physical, mechanical, chemical, or biological) found in each one are reported. From Table 4, it can be noted that the fort has been mostly affected in terms of its aesthetic, while mechanical damage is observed in the fort sectors where structure stability is compromised.

Design quality coefficient (Φ_{dc}) were considered equal to 0.8 and uniformly applied to the measured mechanical properties to obtain the design parameters. On the other hand, material decay reduction coefficient (Φ_{md}) was considered according to the decay classification, 0.6 poor or bad, 0.8 fair and 1.0 good.

This fort has a series of vaults of different types, circular, lancet, depressed and even Ottoman Gothic, [26]. Among the most relevant damage reported are microkarstification and alveolarization with cavities greater than 2 cm, wall deterioration, and a loss of stone material. Additionally, the proliferation of fungi and efflorescence was identified, probably related to the high moisture content in the material, (Fig. 7). Salt crystallization, thermal stresses, differential water expansion, and biological growth likely play an important role in the decomposition of wall materials.

Only the most severe combination (Case 6 - Soil-structure interaction) was reported in the results, given that overstress rate (OR) related to the other cases are significantly lower than 1 (<0.3). OR were calculated according to Eqs. (1) and (2).

$$OC_R = \frac{AC_s}{UCS_{mb}} \tag{2}$$

$$OS_R = \frac{AS_s}{S_{ms}} \tag{3}$$

Where OC_R and OS_R are respectively the Compressive Overstress rate and the Shear Overstress rate (adim.), resulting from the applied stress divided by the resistant stress. Accordingly, AC_S is the Applied Compressive Stress (MPa), and AS_S is the Applied Shear Stress (MPa).

The masonry uniaxial compressive strength values due to bending (UCS_{mb} in MPa) and Shear Strength (S_{ms} in MPa), were calculated according to the NSR, 2010 (3). For further details see Saba et al. [37].

When the Overstress rate is lower than 1, the structure response is considered adequate to the combination load applied, otherwise, the structure will have criticalities and risk of collapse.

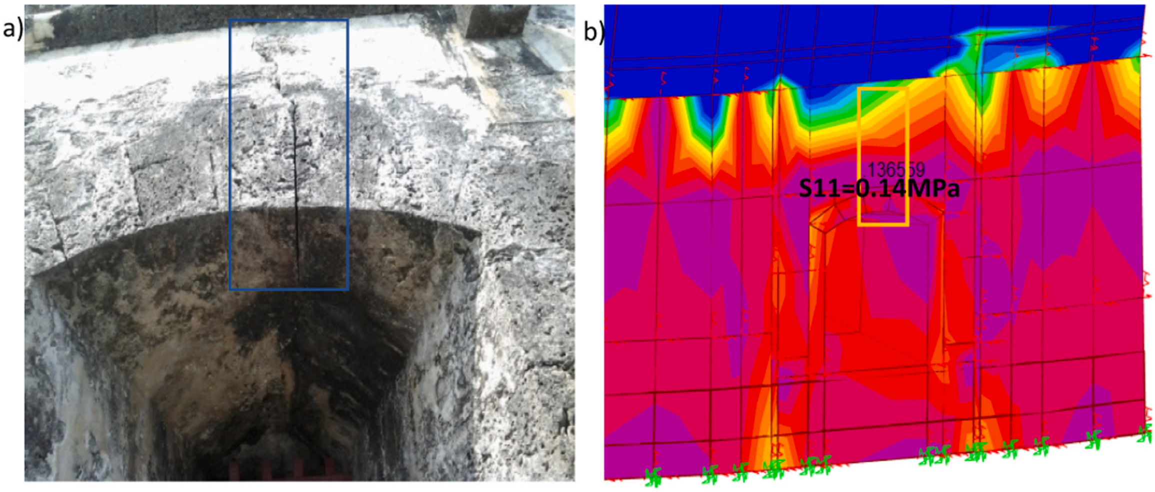

Fig. 8. a) Crack in the stone material in the upper part of a window, up to 2 cm thick in the real structure; b) state of stress resulting from numerical modeling with SAP2000.

Fig. 9. Scour and deterioration of the stone material in the external part of the bathroom.

Considering the worst scenario, as mentioned above, the structure has compression overstress indexes lower than 1. This means that all materials are performing well under these stresses. On the other hand, in the case of tensile and shear stresses, the overstress index diagrams show values greater than 1 in all materials, with the highest value being in the section where the material is military brick.

In general terms, it can be affirmed that tensile and shear stresses are producing the greatest stresses on the structure. Additionally, some severe cracks were observed, such as that shown in Fig. 8a, which was up to 2 cm thick. These are probably the consequence of tensile stresses generated in the vault keystone by movements of the ground. The arch in this case is made of limestone, while in its upper part, the material is mixed concrete. In the absence of experimental data, the literature indicates that the Rt of the materials is between 5% and 10% of Rc [37,41,5,9], (Table 1). Observing the numerical modeling, the stress distribution in the vault key of the arch indicates that there is relatively low tensile stress (0.14 MPa; Fig. 8b). However, this request is higher than the Rt range of mixed concrete, (Table 1), justifying the cracking. On the other hand, in limestone, the fracture is occurring in the vicinity of the joint mortar between blocks. In this case, the presence of overstrain in this material could have generated acceleration in its deterioration due to weathering.

As encountered in Saba et al. [37] in previous studies of the Cartagena's fortifications, the main failure mechanism highlighted in the analysis was a local overturning mechanism [19]. The out-of-plane actions, due to bending moments, are often prevalent and represent the most critical situations from a structural point of view. The connection between walls and horizontal elements is not clear, therefore, the typical box-type structural behavior is not effective to avoid the collapse for out-of-plane actions.

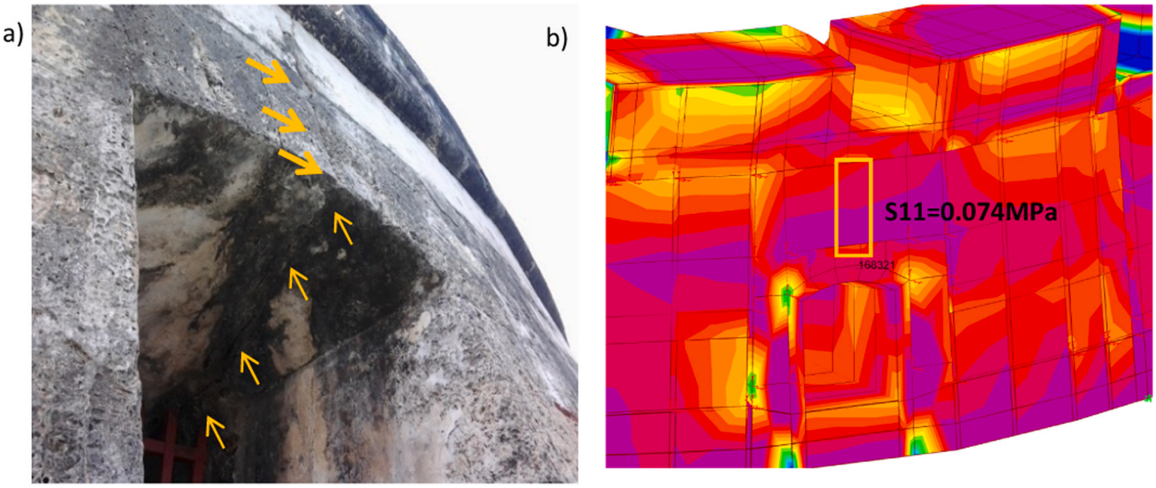

Fig. 10. a) Cracks in the key stone of the bathroom window; b) distribution of stresses according to the numerical simulation with SAP2000 in the same area.

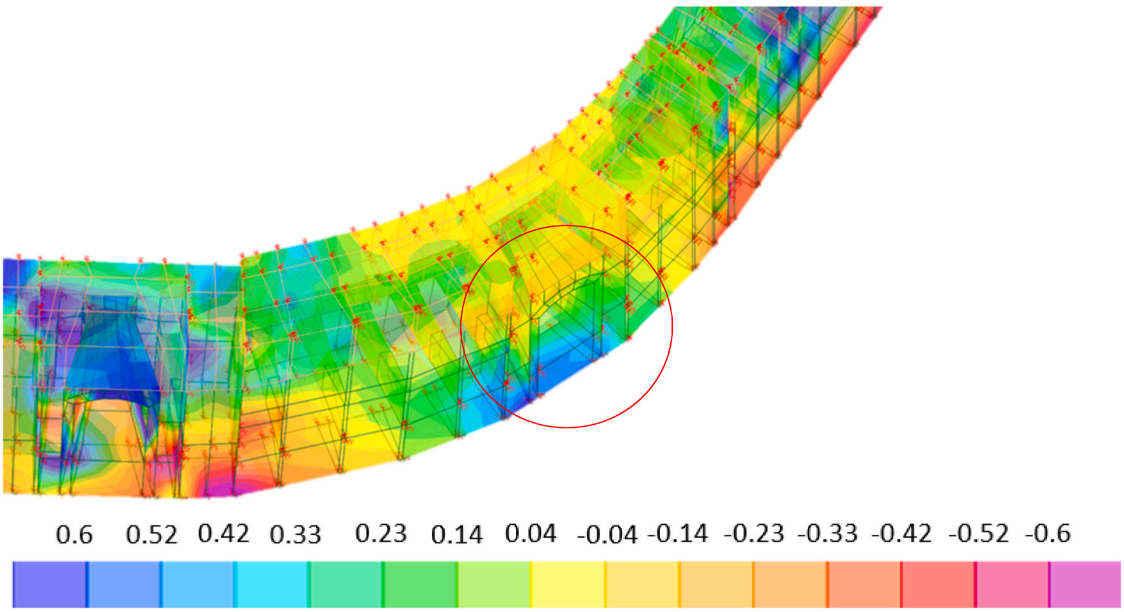

Fig. 11. Overstress diagrams showing the concentration of shear stresses in the lower part of the wall (MPa) [3]. Positive values: traction; negative values: compression.

One of the sectors of the fort where more serious damage was identified was the bathroom (Sector B O1, Fig. 2). It was observed a significant deterioration of the stone material at the base (Fig. 9). This is probably the product of mechanical aggression, the dissolution of salts, and the continuous impact of the sea waves. Cracks were also identified in the key of the bathroom window due to overstressing or settlements produced by the loss of supporting soil. The latter could be a consequence of the action of the sea waves (Fig. 10a,b), a behavior similar to that seen in Fig. 8.

The model shows that the causes of the cracks rely on several factors, including overstresses, scour by water, and the geometry of the vault. The vault does not work as a single compact section, and it has shapes designed for the bathroom drainage system's functionality. This design produced unsupported areas, and it allows for the appearance of cracks (Fig. 11).

Paradiso et al. [26] also report the pattern of cracks present in this sector. This is a large, deep opening that runs the entire length of the floor. The crack continues to the exterior wall and, seeking the weaker areas of masonry, breaks the right edge of the windowsill. Starting from the corner stone of the window arch, the crack resumes, breaking the window and thus causing an interior joint restriction, which continues up to the vaulted ceiling, (Fig. 12a,b).

In the escarpment, similar cracks are found (Fig. 13a,b), which are caused by tensile strength in the battery brick, probably as a

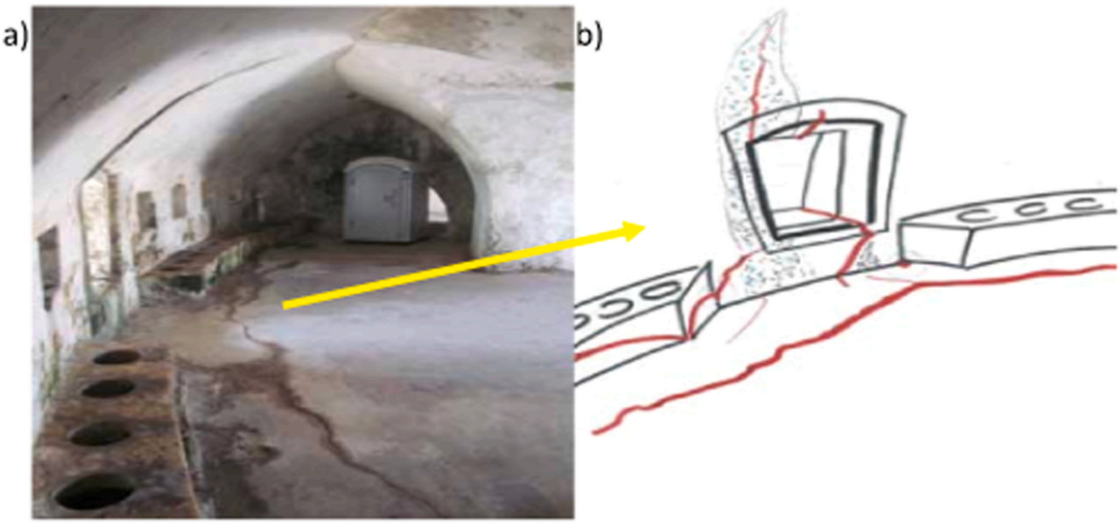

Fig. 12. a) Cracking pattern of the bathroom; b) side view of Fig. 11a). Cracking chart sketch was recovered from Michele Paradiso et al. [26].

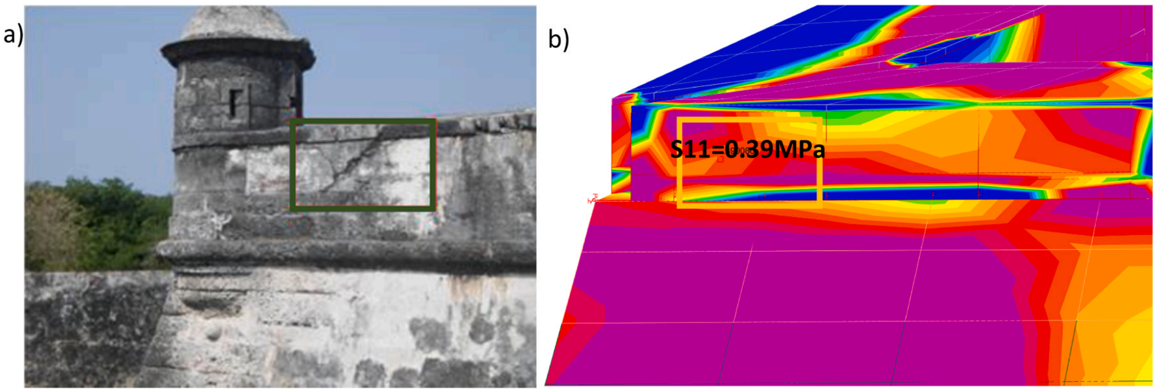

Fig. 13. a) Crack in the scarp with an incline of approximately 45 degrees; b) stresses found in the model in the same area.

consequence of differential settlements. In addition to the above damage, in general, the scarp in its different areas shows increased roughness, alveolarization and microkarstification, as well as partial loss of matrix.

The relationship between the overstress and cracks is evident when considering the fact that military brick Rt oscillates between 0.18 and 0.37 MPa (Table 1), showing compatibility between the model and the real structure.

Most of the studies in historical structures in developing countries are done with few tools as in the present case, so it is a typical case that can be considered as an example for other case studies when there is a lack of funds and logistics.

4. Conclusions

The objective of the present work was to identify the relationship between the decay process and damage in San Fernando de Bocachica Fort, Cartagena de Indias. The results show that, in most of the walls and vaults, there is a predominance of biological material (molds and fungi), probably as a consequence of the high moisture content propitiated by the proximity to the sea and the poor state of the rainwater drains. Among the damage processes identified, "features induced by loss of material" are prevalent, mainly highlighting the disjunction of films and the increase in roughness. However, the most severe damage is found in the bathrooms. The formation of cracks, among other things, can lead to the infiltration of moisture and pollutants, in turn favoring the formation of other decay processes and worsening the general condition of the structure. Additionally, a relationship was found between the largest cracks and the greatest stress distribution in specific points of the structure. This shows that, with a good level of knowledge of the properties of the materials and appropriate numerical simulation of the structural behavior, the most vulnerable points of the structure can be predicted where cracks and fissures are most likely to appear. Therefore, when competent authorities plan the maintenance and restoration of cultural heritage, they should consider both decay processes and structural behavior. Particularly, in the case of this study, it is considered urgent to take the appropriate actions throughout the entire fort to avoid collapses and the loss of invaluable heritage. This approach is advisable to better preserve cultural heritage around the world.

Declaration of Competing Interest

The authors declare that they have no known competing financial interests or personal relationships that could have appeared to influence the work reported in this paper.

Acknowledgements

The authors owe a special thanks to the Ministry of Culture of Colombia to allow access to the structure.

References

[1] S. Baraccani, M. Palermo, G. Gasparini, T. Trombetti, A time domain approach for data interpretation from long-term static monitoring of historical structures, Struct. Control Health Monit. 28 (5) (2021), e2708, https://doi.org/10.1002/stc.2708.
[2] S. Baraccani, S. Silvestri, G. Gasparini, M. Palermo, T. Trombetti, E. Silvestri, R. Lancellotta, A. Capra, A structural analysis of the modena cathedral, Int. J. Archit. Herit. 10 (2–3) (2016) 235–253, https://doi.org/10.1080/15583058.2015.1113344.
[3] A. Berrocal Olave, 2018. Evaluación patológica de la vulnerabilidad sísmica y efectos del oleaje en el fuerte-batería de San José y San Fernando de Bocachica.
[4] S. Boschi, A. Borghini, B. Pintucchi, N. Zani, Seismic vulnerability of historic masonry buildings: a case study in the center of Lucca, Proc. Struct. Integr. 11 (2018) 169–176, https://doi.org/10.1016/j.prostr.2018.11.023.
[5] A. Brencich, 2020. Elementi costitutivi del ponte. http://profgiuseppeclemente.altervista.org/alterpages/files/costruzioni_quinta/Ponti/ponti_in_muratura_Universit__Genova.pdf.
[6] J. Catalá, P. Calderón, 2014. Estudios y diseños integrales a fase iii para la ejecución de las obras de reforzamiento estructural y protección perimetral del fuerte San Fernando y el fuerte batería San José en bocachica, en la ciudad de Cartagena, departamento de Bolívar.
[7] I. Catapano, A. Affinito, L. Guerriero, B. Bisceglia, F. Soldovieri, Majolica imaging with THz waves: preliminary results, Appl. Phys. A Mater. Sci. Process. 122 (533) (2016), https://doi.org/10.1007/s00339-016-0055-2.
[8] R. Ceravolo, A. De Marinis, M.L. Pecorelli, L. Zanotti Fragonara, Monitoring of masonry historical constructions: 10 years of static monitoring of the world's largest oval dome, Struct. Control Health Monit. 24 (10) (2017), e1988, https://doi.org/10.1002/stc.1988.
[9] F. Ceroni, M. Di Ludovico, Traditional and innovative systems for injected anchors in masonry elements: experimental behavior and theoretical formulations, Constr. Build. Mater. 254 (2020), 119178, https://doi.org/10.1016/j.conbuildmat.2020.119178.
[10] X. Chen, B. Hofland, W. Molenaar, A. Capel, M.R.A. Van Gent, Use of impulses to determine the reaction force of a hydraulic structure with an overhang due to wave impact, Coast. Eng. 147 (2019) 75–88, https://doi.org/10.1016/j.coastaleng.2019.02.003.
[11] Á. Covo, 2012. Teoría del ángulo de fricción interna bidimensional en arenas. 7,1, 7–24.
[12] A. Dandge, S. Valsson, Conservation of material, technology and practice in heritage structure and its relevance in today's context, Encycl. Renew. Sustain. Mater. (2020) 39–49, https://doi.org/10.1016/b978-0-12-803581-8.10723-4.
[13] T. de Rubeis, I. Nardi, M. Muttillo, D. Paoletti, The restoration of severely damaged churches – implications and opportunities on cultural heritage conservation, thermal comfort and energy efficiency, J. Cult. Herit. 43 (2019) 186–203, https://doi.org/10.1016/j.culher.2019.11.008.
[14] L.C. Fecundo Sanches, Uma Resolucao de Placas Com a teoria de Mindlin Atra ves do Metodo dos Elementos de Contorno, Universidade Estadual de Campinas, Facultade de Engenharia Civil, Brazil, 1998.
[15] S. Grecu, L.B. Ibsen, A. Barari, Winkler springs for axial response of suction bucket foundations in cohesionless soil, Soils Found. 61 (1) (2021) 64–79, https://doi.org/10.1016/j.sandf.2020.10.010.
[16] Hidroconsultores Ltda., 2012. Estudios oceanográficos y de la dinámica costera y diseños de las alternativas de protección costera a los fuertes de San Fernando y San José en el canal de acceso a la bahía de Cartagena.
[17] ICOMOS-ISCS, 2008. Illustrated glossary on stone deterioration patterns (XV).
[18] C. Isla Vallejos, M. Nozaki Uribe, C, O. V., 2017. Simposio de Habilitación Profesional: Departamento de Ingeniería Civil. Modelación y Análisis Modal Con Elementos Sólidos En SAP2000 de Un Muro de Albañilería Sin Reforzar, 1–22.
[19] K. Kaptan, Shear failure of historic masonry walls, Bitlis Eren Univ. J. Sci. Technol. 6 (1) (2016) 1–6, https://doi.org/10.17678/beujst.27782.
[20] Y.S. Kuo, C.S. Lin, C.Y. Chung, Y.K. Wang, Wave loading distribution of oscillating water column caisson breakwaters under non-breaking wave forces, J. Mar. Sci. Technol. 23 (1) (2015) 78–87, https://doi.org/10.6119/JMST-014-0114-1.
[21] P.B. Lourenço, Computations on historic masonry structures, Progress Struct. Eng. Mater. 4 (3) (2002) 301–319, https://doi.org/10.1002/pse.120.
[22] N. Makoond, L. Pelà, C. Molins, P. Roca, 2020. SPIE Smart Structures and Materials + Nondestructive Evaluation and Health Monitoring. Static Structural Health Monitoring and Automated Data Analysis Procedures Applied to the Diagnosis of a Complex Medieval Masonry Monastery, 11379. https://doi.org/10.1117/12.2559837.
[23] M.-G. Masciotta, L.F. Ramos, P.B. Lourenco, The importance of structural monitoring as a diagnosis and control tool in the restoration process of heritage structures: a case study in Portugal, J. Cult. Herit. 27 (2017) 36–47, https://doi.org/10.1016/j.culher.2017.04.003.
[24] M.G. Masciotta, L.F. Ramos, P.B. Lourenço, J.A. C. Matos, 2016. 8th European Workshop on Structural Health Monitoring (EWSHM 2016), July 5–8, 2016 in Bilbao, Spain (EWSHM 2016). Development of Key Performance Indicators for the Structural Assessment of Heritage Buildings. https://www.ndt.net/search/docs.php3?id=20121.
[25] F. Micelli, A. Cascardi, Structural assessment and seismic analysis of a 14th century masonry tower, Eng. Fail. Anal. 107 (104198) (2020), https://doi.org/10.1016/j.engfailanal.2019.104198.
[26] Michele Paradiso, Florencia, U.De, Florencia, U.De, Florencia, U.De, 2013. San Fernando De Bocachica, Cartagena De a Contribution To Knowing Fort San. 10, 2, 136–158.
[27] G. Milani, P.B. Lourenço, A simplified homogenized limit analysis model for randomly assembled blocks out-of-plane loaded, Comput. Struct. 88 (2010) 690–717, https://doi.org/10.1016/j.compstruc.2010.02.009.
[28] MitCIT, 2017. Boletin Mensual Turismo Noviembre 2017 - Ministerio de Comercio Industria y Turismo, Oficina de estudios economicos - Colombia. http://www.mincit.gov.co/minturismo/eventos-y-publicaciones/boletin-informativo-del-sector-turismo.
[29] D. Navas-Carrillo, J. Navarro-De-Pablos, Patrimonio mundial y desarrollo sostenible: ¿hacia un nuevo modelo de gestión? EURE 46 (138) (2020) 257–261, https://doi.org/10.4067/s0250-71612020000200257.
[30] P. Pachón, M. Infantes, M. Cámara, V. Compán, E. García-Macías, M.I. Friswell, R. Castro-Triguero, Evaluation of optimal sensor placement algorithms for the Structural Health Monitoring of architectural heritage. Application to the Monastery of San Jerónimo de Buenavista (Seville, Spain), Eng. Struct. 202 (2020), 109843, https://doi.org/10.1016/j.engstruct.2019.109843.
[31] D. Reale, C. Noviello, S. Verde, L. Cascini, G. Terracciano, L. Arena, A multi-disciplinary approach for the damage analysis of cultural heritage: the case study of the St. Gerlando Cathedral in Agrigento, Remote Sens. Environ. 235 (October) (2019), 111464, https://doi.org/10.1016/j.rse.2019.111464.
[32] J.M. Reinosa, L.E. Romera, Stability of megalithic structures against overturning, J. Cult. Herit. 16 (6) (2015) 798–804, https://doi.org/10.1016/j.culher.2015.03.006.

[33] F. Ribera, A. Nesticò, P. Cucco, G. Maselli, A multicriteria approach to identify the highest and best use for historical buildings, J. Cult. Herit. 41 (2020) 166–177, https://doi.org/10.1016/j.culher.2019.06.004.

[34] P. Roca, M. Cervera, G. Gariup, L. Pela', Structural analysis of masonry historical constructions. Classical and advanced approaches, Arch. of Comput. Methods Eng. 17 (3) (2010) 299–325, https://doi.org/10.1007/s11831-010-9046-1.

[35] P. Roca, J.L. Gonzàles, E. Oñate, P.B. Lourenço, P.P. Rossi, C. Rossi, Surveillance and monitoring of ancient structures: recent developments, Struct. Anal. Hist. Construct. II (1998) 1–15.

[36] M. Saba, N. Hernandez-Romero, E. Quiñones-Bolaños, J. Lizarazo-Marriaga, Petrographic of limestone cultural heritage as the basis of a methodology to rock replacement and masonry assessment: cartagena de indias case of study, Case Stud. Construct. Mater. 11 (2019), e00281, https://doi.org/10.1016/j.cscm.2019.e00281.

[37] M. Saba, J.M. Lizarazo-Marriaga, E. Quiñones-Bolaños, Overstress analysis of the Cartagena de Indias walls under different scenarios of masonry mechanical strength, Case Stud. Construct. Mater. 13 (2020), e00410, https://doi.org/10.1016/j.cscm.2020.e00410.

[38] G. Sainflou, Essai sur les digues maritimes verticales, Annales Ponts Chaussées 98 (4) (1928) 5–48 tome II.

[39] R. Segovia, 1998. The Fortifications of Cartagena de Indias: Strategy and History (El Ancora Editores (ed.)). El Ancora Editores.

[40] UNESCO. (1984). Port, Fortresses and Group of Monuments, Cartagena, Colombia. https://whc.unesco.org/archive/repcom84.htm.

[41] J. Vemuri, S. Ehteshamuddin, M. Ravula, S. Kolluru, Pushover analysis of soft brick unreinforced masonry walls using analytical and numerical approaches, Mater. Today Proc. 28 (2019) 420–425, https://doi.org/10.1016/j.matpr.2019.10.025.

[42] S. Xiao, P. Xia, Variational calculus method for passive earth pressure on rigid retaining walls with strip surcharge on backfills, Appl. Math. Model. 83 (2020) 526–551, https://doi.org/10.1016/j.apm.2020.03.008.

[43] J.W. Yun, J.T. Han, Evaluation of soil spring methods for response spectrum analysis of pile-supported structures via dynamic centrifuge tests, Soil Dyn. Earthq. Eng. 141 (2021), 106537, https://doi.org/10.1016/j.soildyn.2020.106537.